NACA RM No. E8J22a

NACA

RESEARCH MEMORANDUM

VIBRATION SURVEY OF BLADES IN 10-STAGE AXIAL-FLOW COMPRESSOR

II - DYNAMIC INVESTIGATION

By André J. Meyer, Jr.
and Howard F. Calvert

Lewis Flight Propulsion Laboratory
Cleveland, Ohio

NATIONAL ADVISORY COMMITTEE
FOR AERONAUTICS

January 31, 1949

NATIONAL ADVISORY COMMITTEE FOR AERONAUTICS

RESEARCH MEMORANDUM

VIBRATION SURVEY OF BLADES IN 10-STAGE AXIAL-FLOW COMPRESSOR

II - DYNAMIC INVESTIGATION

By André J. Meyer, Jr.
and Howard F. Calvert

SUMMARY

Strain-gage measurements were taken under operating conditions from blades of various stages of an axial-flow compressor in an effort to determine the reason for failures in the seventh and tenth stages. First bending-mode vibrations were detected in the first five stages of the compressor caused by each integral multiple of rotor speed from three through ten. Lead-wire failures in the last five stages resulted in incomplete data. The dynamic-vibration frequencies at various rotor speeds were compared with statically measured frequencies analytically corrected for the influence of centrifugal force. Large increases in vibration amplitude with increased pressure ratio were observed. During surging operation, blade vibrations were not present. The effects of pressure ratio and surge indicate the existence of aerodynamic excitation as the cause of the blade vibrations.

INTRODUCTION

An investigation is being conducted at the NACA Lewis laboratory to determine the cause of failures, reported by the manufacturer, of the seventh- and the tenth-stage blades in an early experimental model of a 10-stage axial-flow compressor. Natural-frequency measurements, node-shape determinations, and critical-speed diagrams for each of the 10 stages of the rotor under static conditions are included in reference 1. From the static investigation (reference 1), the conclusion was reached that the failures reported could have resulted from fourth-order and sixth-order exciting forces for the seventh and tenth stages, respectively.

Vibratory-stress and frequency determinations at operating conditions by the use of strain gages mounted on the blades are reported herein. The purpose of these dynamic experiments was to detect existing exciting forces and to evaluate their order or multiple of rotor speed. The effects of surge and of changes in pressure ratio on amplitude of blade vibrations were also investigated. Curves are presented that compare the values of vibration frequency measured under operating conditions with the values predicted for these conditions by correcting statically measured values for the effect of centrifugal force.

APPARATUS AND PROCEDURE

For checking purposes, 36 active strain-gage bridges were mounted on blades of the various stages with at least two bridges per stage. The gages were mounted on the blades with Bakelite cement with the resistance-wire filaments parallel to the direction of maximum compressive and tensile stresses for the mode of vibration in question (fig. 1). Some of the gages were used to detect bending vibrations and others to detect torsional vibrations. The construction of the gages is similar to that outlined in reference 2.

The lead wires were silk-covered, enameled, No. 27 copper wire with three additional coats of thermal-setting varnish. These wires were pulled through holes drilled in the rotor as shown in figure 2 and connected to the slip-ring assembly (fig. 3). A schematic diagram of the strain-gage circuit used for measuring vibratory stresses is presented in figure 4; three circuits similar to the one illustrated were installed, which permitted 12 signals to be recorded simultaneously by the 12-channel amplifier and oscillograph. By means of a special switching arrangement incorporated in the slip-ring assembly, any set of strain gages could be connected to the recording instruments in a few minutes. Strain gages similar to the active gages were used as balancing resistors and were placed on the periphery of the rotor disks with the filaments parallel to the axis of the rotor.

Insulation on the lead wires was safeguarded by smoothing the holes drilled in the rotor and by rounding the junctions of the holes by use of a liquid honing process. The wires were firmly embedded in a ceramic cement that was forced into the holes after the wires were pulled into position and attached to the strain gages. A lead-shielded telephone cable completed the circuit from the slip rings to the instruments located in a control room adjacent to the test cell.

The compressor, tested separately from the other parts of the engine, was driven through a variable-speed magnetic coupling and speed increasers by a 2500-horsepower constant-speed drive motor (fig. 5). The compressor intake was open to the atmosphere but the compressed air was exhausted into a controlled pressure system. The compressor pressure ratio was varied by means of a butterfly valve in the exhaust line.

Compressor rotor speed was varied until vibration signals were observed at which time photographic data were recorded. The magnitude of the vibratory stresses was evaluated by comparison with stress signals of known magnitude supplied from similar strain gages mounted on the bar of a calibrating instrument.

The operating range of the equipment was limited to a compressor speed of 14,000 rpm by lack of driving power, although the compressor is rated at 17,000 rpm. Unfortunately, conclusive data on the last five stages were not obtained because some of the lead wires were thrown out by centrifugal force during the elapsed running time needed to eliminate instrumentation difficulties. The lead-wire failures were attributed to poor adhesion and faulty void filling by the ceramic cement.

RESULTS AND DISCUSSION

The results of the static frequency measurements made on blades of the compressor indicated that failures experienced in the seventh and tenth stages could have been caused by first bending-mode vibrations resulting from fourth- and sixth-order excitation of the rotative speed, respectively. Critical-speed diagrams illustrating this possibility are included in reference 1. The sources of the fourth- and sixth-order exciting forces have not been learned. Although four bearing supports interrupt the inlet-air stream, it is doubtful that the effect of these supports would carry as far as the seventh stage. No condition exists within the compressor that would cause six equally spaced discontinuities in the air flow.

During compressor operation at low pressure ratios (atmospheric inlet and exhaust pressure), sharply resonant blade vibrations were observed as the rotative speed was changed. Analysis revealed that the critical speeds were exact multiples of the first bending-mode frequencies of the blades. Actually after two resonant speeds were known, a critical-speed diagram was drawn from which other critical speeds were predicted (fig. 6). Oscillograph records were taken at each critical speed and were analyzed to determine frequency, order, and magnitude of the vibratory stresses. Figure 7 shows representative

strain-gage signals from first- and fifth-stage blades that happened to resonate at the same rotor speed (9485 rpm). The vibration of the first-stage blade caused by a third-order excitation was 477 cycles per second and the measurements showed a total vibratory stress of 3700 pounds per square inch at the location of the gage. The conditions for the fifth-stage blade were a vibration of 794 cycles per second, a fifth-order excitation, and a vibratory stress of 3000 pounds per square inch. The following table gives the orders of rotor speed that were detected in the form of first bending-mode vibrations of blades in the first five stages:

Stage	Order of rotor speed
1	3, 4, 5, and 6
2	3, 4, 5, 6, and 7
3	4, 5, 6, 7, and 8
4	4, 5, 6, 7, and 8
5	4, 5, 6, 7, 8, 9, and 10

Lead-wire failures occurred before data were obtained for the continuation of this list for the other stages.

The second bending mode of blade vibrations was detected in only the first stage and no torsional vibrations were picked up by the strain gages.

The first bending-mode frequencies, as determined from the oscillograph records, are shown plotted against rotor speed in figure 8. The curves of the statically measured natural frequencies corrected for the effect of centrifugal force in accordance with reference 3 are also shown on the figure. An average line drawn through the experimental resonant points has a slightly lower slope than the calculated line. This discrepancy is probably due to the variance between the fixed blade mount assumed for the calculations and the actual bulbous-root mounting arrangement used throughout the compressor. Also, the assumed deflection curve used in the calculations differs from the true deflection curve of the vibrating blade. Figure 8(d) is of special significance because the natural frequencies of two blades of the fourth stage are plotted. Considerable difference in the natural static frequencies of these two blades can be noted. In reference 1, it is stated that at rated speed (17,000 rpm) the frequencies of all blades might approach the highest blade frequency in the stage because the centrifugal

force and thermal expansion raise the frequency by tightening the bulbous blade root. This conclusion, though generally true, is contradicted in the compressor as indicated by figure 8(d) and more clearly by figure 9, which is similar to figure 8 except that different coordinates are used, frequency squared and revolutions per second squared, resulting in straight-line relations. No convergence of lines through data points for the two blades occurs with an increase in speed. This fact was noted in the other stages of the compressor also but the fourth stage was arbitrarily chosen as an example.

The effect of changing pressure ratio of the compressor by throttling the exhaust is clearly shown in figure 10. All gage signals were taken at the same amplification and rotative speed (8190 rpm) at pressure ratios of 1.17 and 1.54. The rotor speed was so set that the signal from stage 2 would be in fourth-order resonance at a pressure ratio of 1.17. The vibration amplitude of the second-stage signal was more than doubled by the pressure-ratio increase; the third- and fourth-stage blades vibrated at 4.65 and 4.72 orders, respectively, at a pressure ratio of 1.54 and did not vibrate at the low pressure ratio. Furthermore, no correlation was apparent between the high and the low amplitudes of the second-, third-, and fourth-stage signals at a pressure ratio of 1.54. These effects of change in pressure ratio were investigated at several other rotative speeds and the same results observed. All stress measurements were comparatively low but the limited driving power did not permit operation at the rated conditions (rotor speed, 17,000 rpm; pressure ratio, 4.0).

When the butterfly valve in the exhaust system was partly closed to attain surging conditions in the compressor, the blade vibrations ceased until the valve was reopened to remove the surging conditions; then the vibrations were resumed.

SUMMARY OF RESULTS

From a preliminary investigation of destructive vibratory stresses present in a 10-stage axial-flow compressor, conducted by means of strain gages mounted on blades of only the first five stages (lead wires failed in other stages), the following results were obtained:

1. First bending-mode vibrations of the blades were detected at each exact multiple of rotor speed from three to ten.

2. A good correlation was obtained between first bending-mode frequencies that were dynamically measured and those that were calculated by correcting static measurements to account for the effects of centrifugal force.

3. Increases in pressure ratio of the compressor greatly increased the amplitude of blade vibrations.

4. Throttling the exhaust of the compressor until surging conditions were reached suppressed existing blade vibrations.

CONCLUSIONS

The presence of fourth- and sixth-order exciting forces in all the stages from which strain-gage signals could be recorded substantiates the theory that failures in the seventh and tenth stages could be caused by these orders.

Although the measured vibratory stresses were low, the stresses at rated speed and pressure ratio may be destructive inasmuch as pressure ratio has a very pronounced effect on vibration amplitude and all reported failures have occurred at high pressure ratios.

The facts that pressure ratio greatly influences the magnitude of the vibratory stresses and that surging suppresses existing vibrations indicate aerodynamic excitation rather than mechanical excitation as the source.

Lewis Flight Propulsion Laboratory,
National Advisory Committee for Aeronautics,
Cleveland, Ohio.

REFERENCES

1. Meyer, André J., Jr., and Calvert, Howard F.: Vibration Survey of Blades in 10-Stage Axial-Flow Compressor. I - Static Investigation. NACA RM No. E8J22, 1949.

2. Kemp, R. H., Morgan, W. C., and Manson, S. S.: The Application of High-Temperature Strain Gages to the Measurement of Vibratory Stresses in Gas-Turbine Buckets. NACA TN No. 1174, 1947.

3. Timoshenko, S.: Vibration Problems in Engineering. D. Van Nostrand Co., Inc., 2d ed., 1937, pp. 383-385.

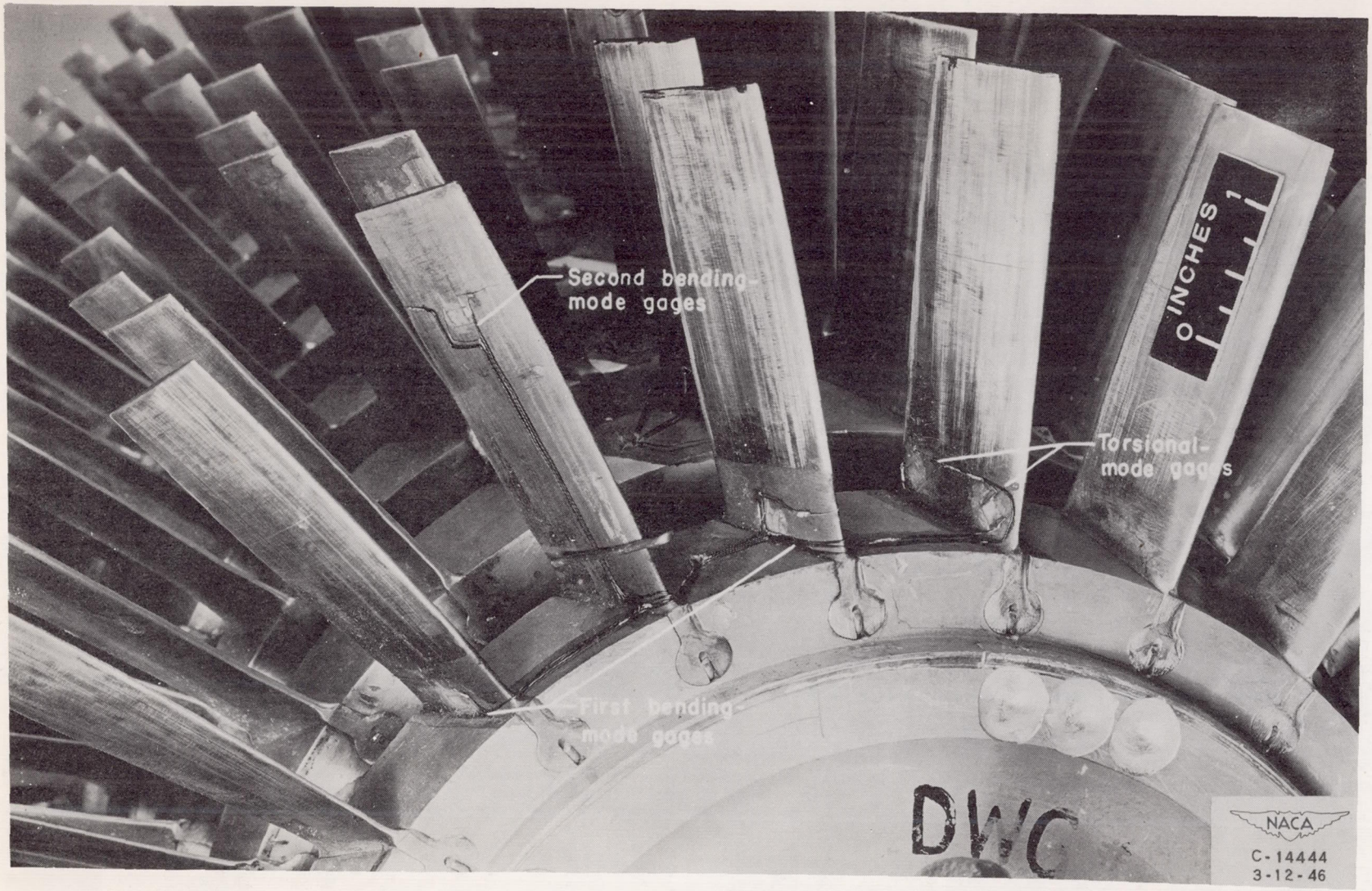

Figure 1. - Strain gages mounted on blades of first stage of 10-stage compressor.

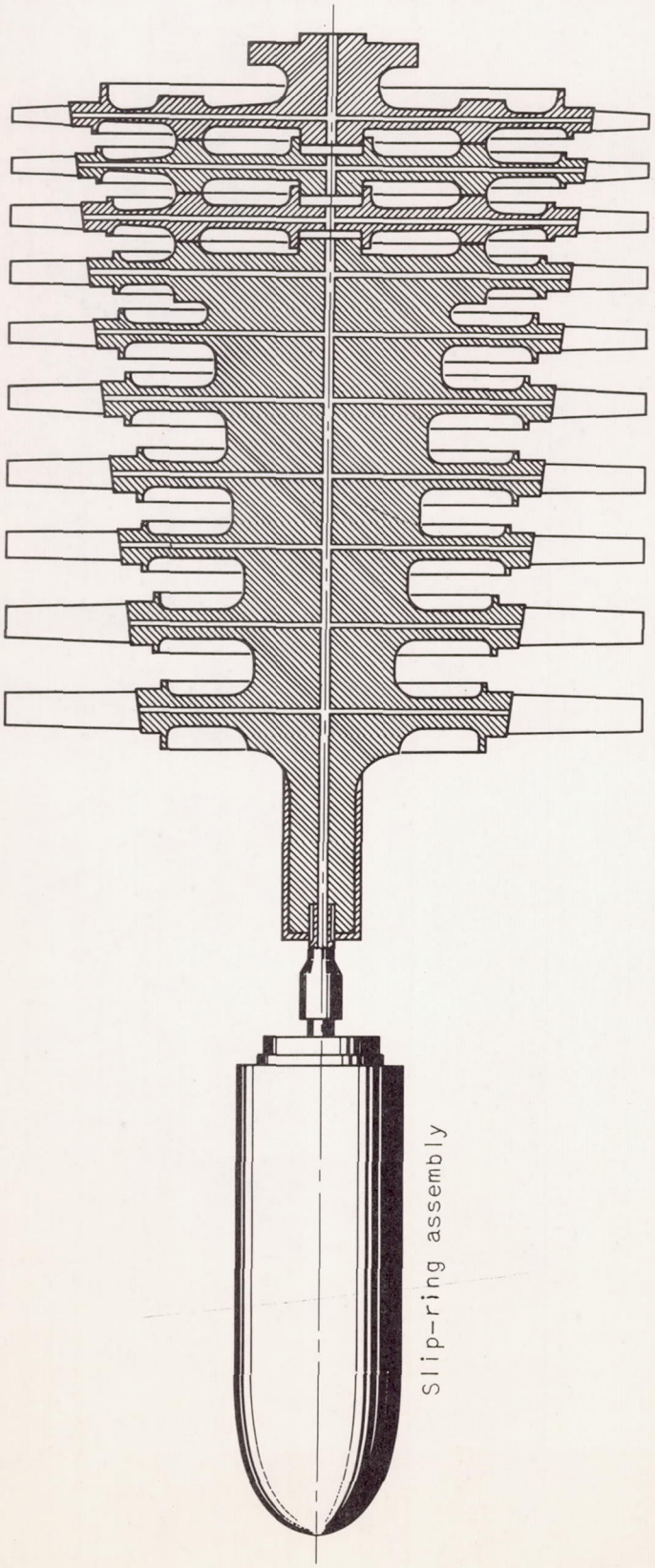

Figure 2. - Axial-flow compressor rotor drilled for strain-gage lead wires.

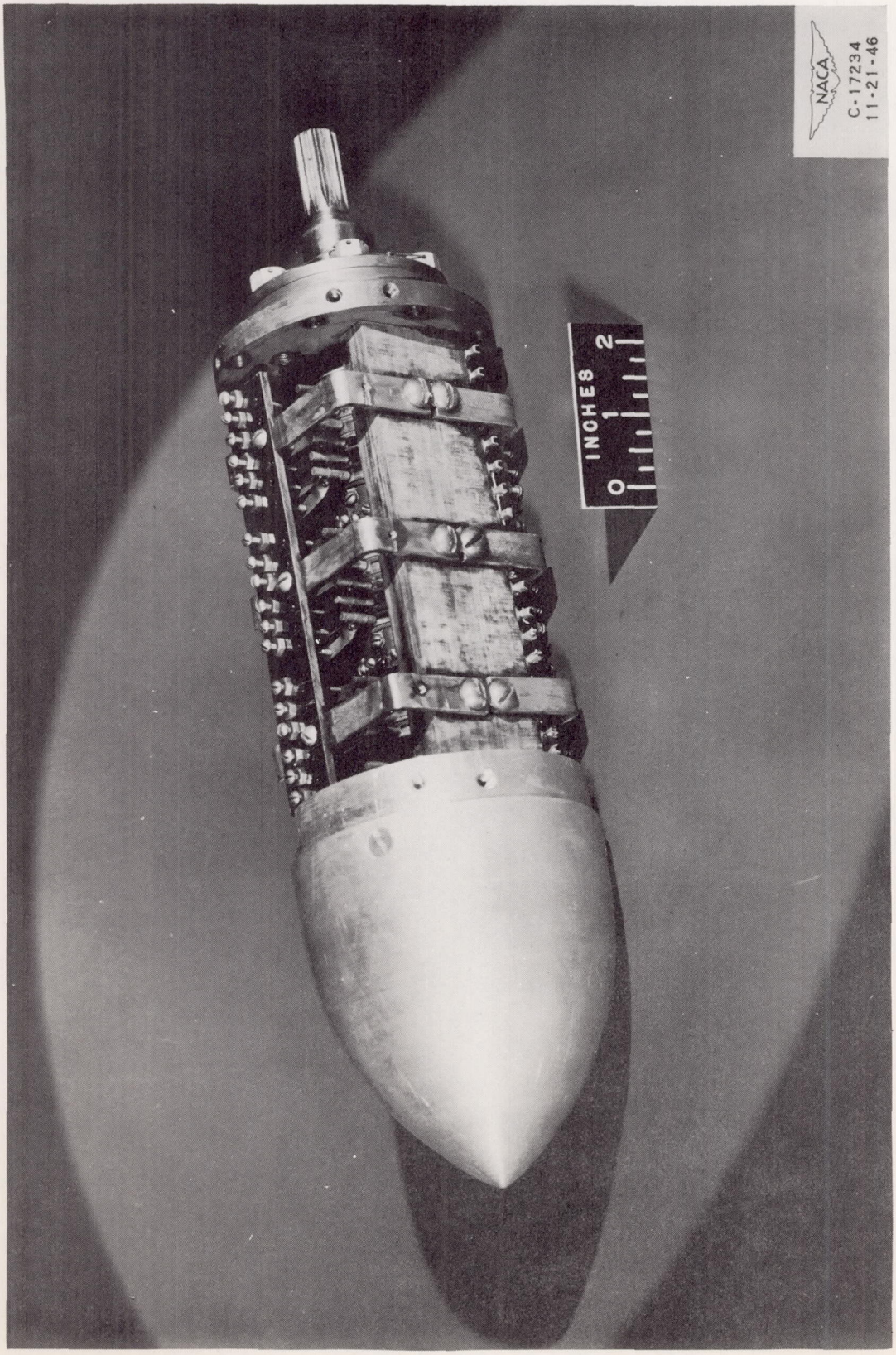

Figure 3. - Slip-ring assembly.

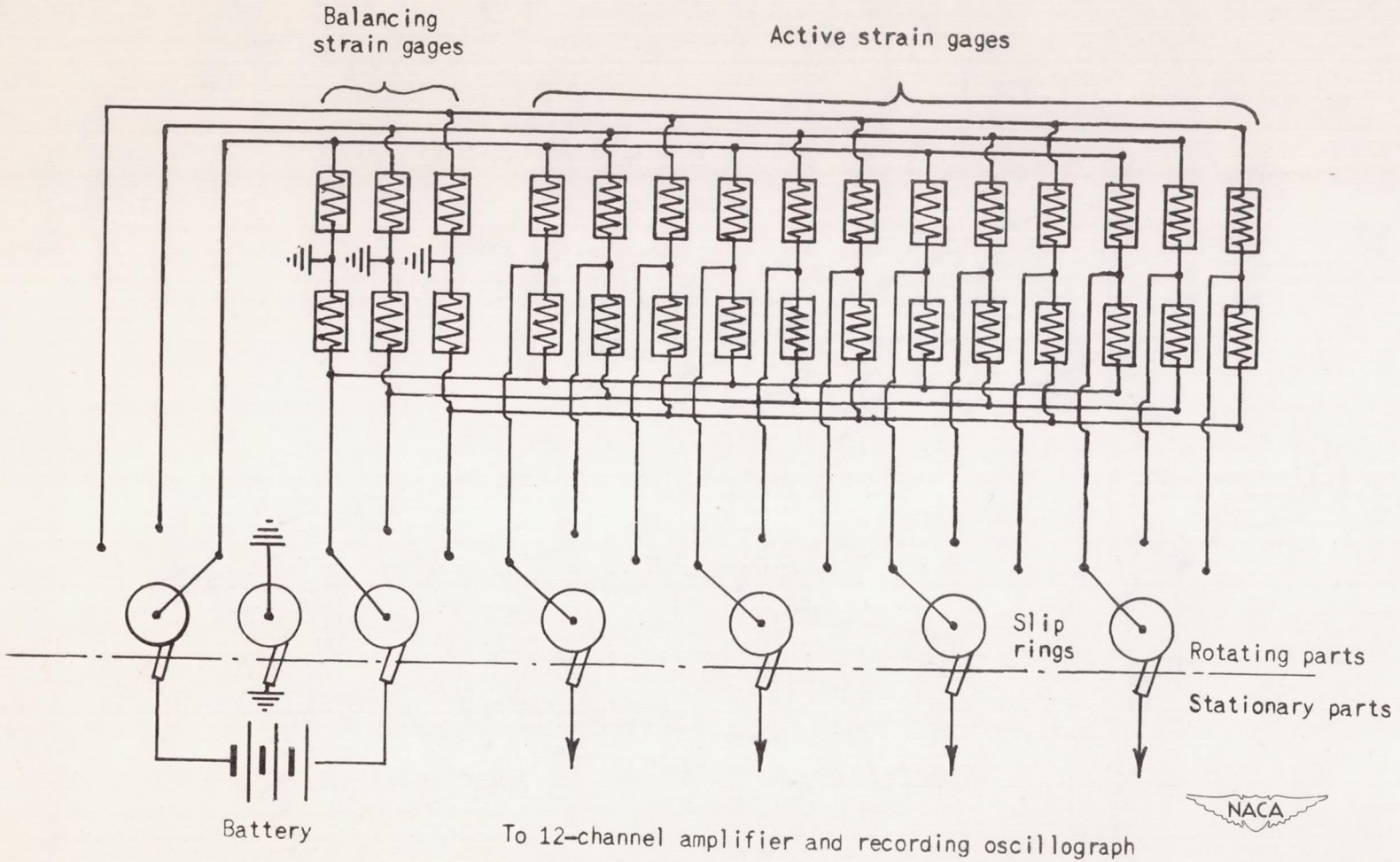

Figure 4. - Schematic diagram of bridge circuit installed on 10-stage axial-flow compressor. Three complete circuits similar to one shown were used in the investigation.

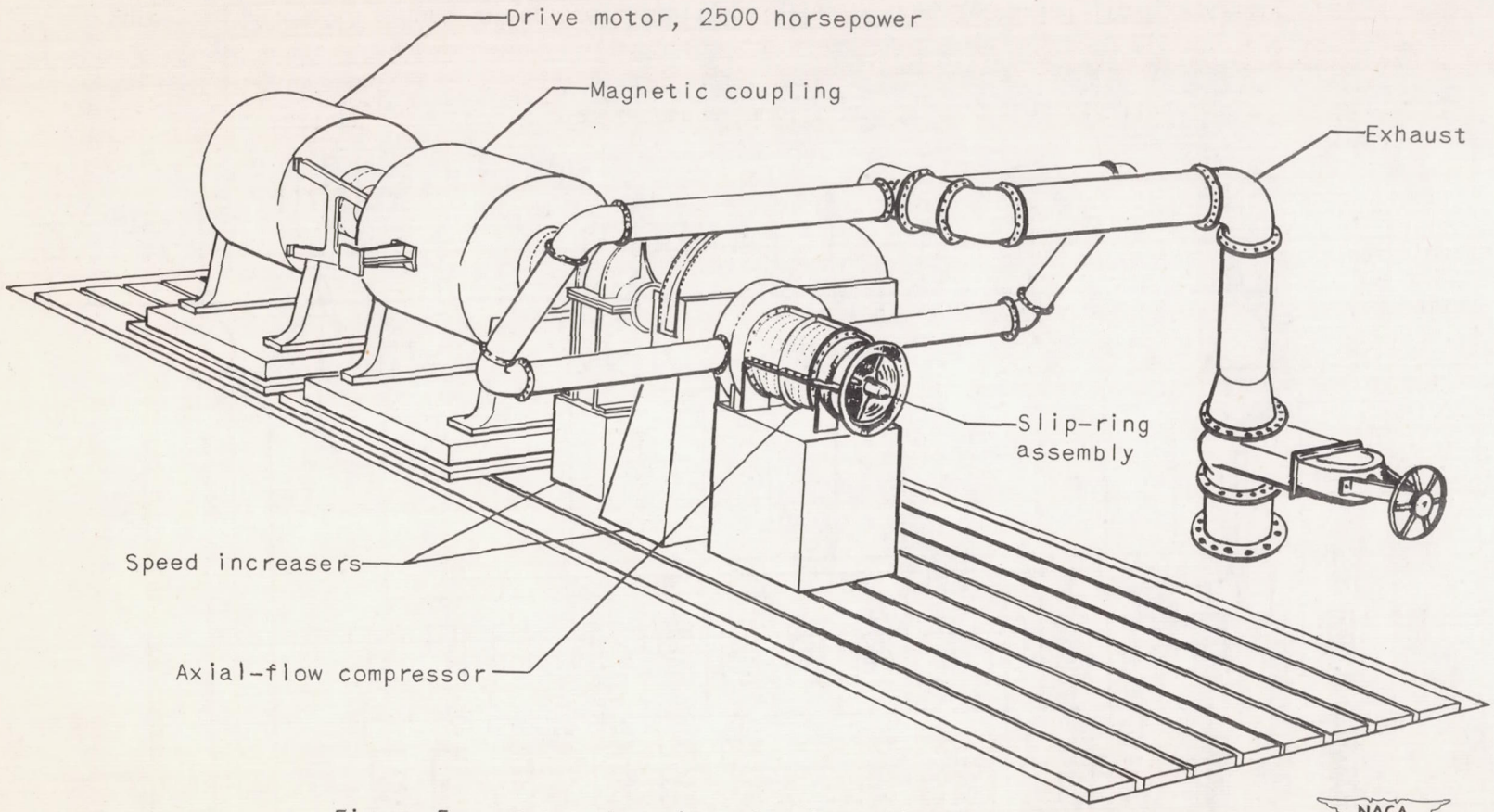

Figure 5. - Setup for vibration investigation of compressor.

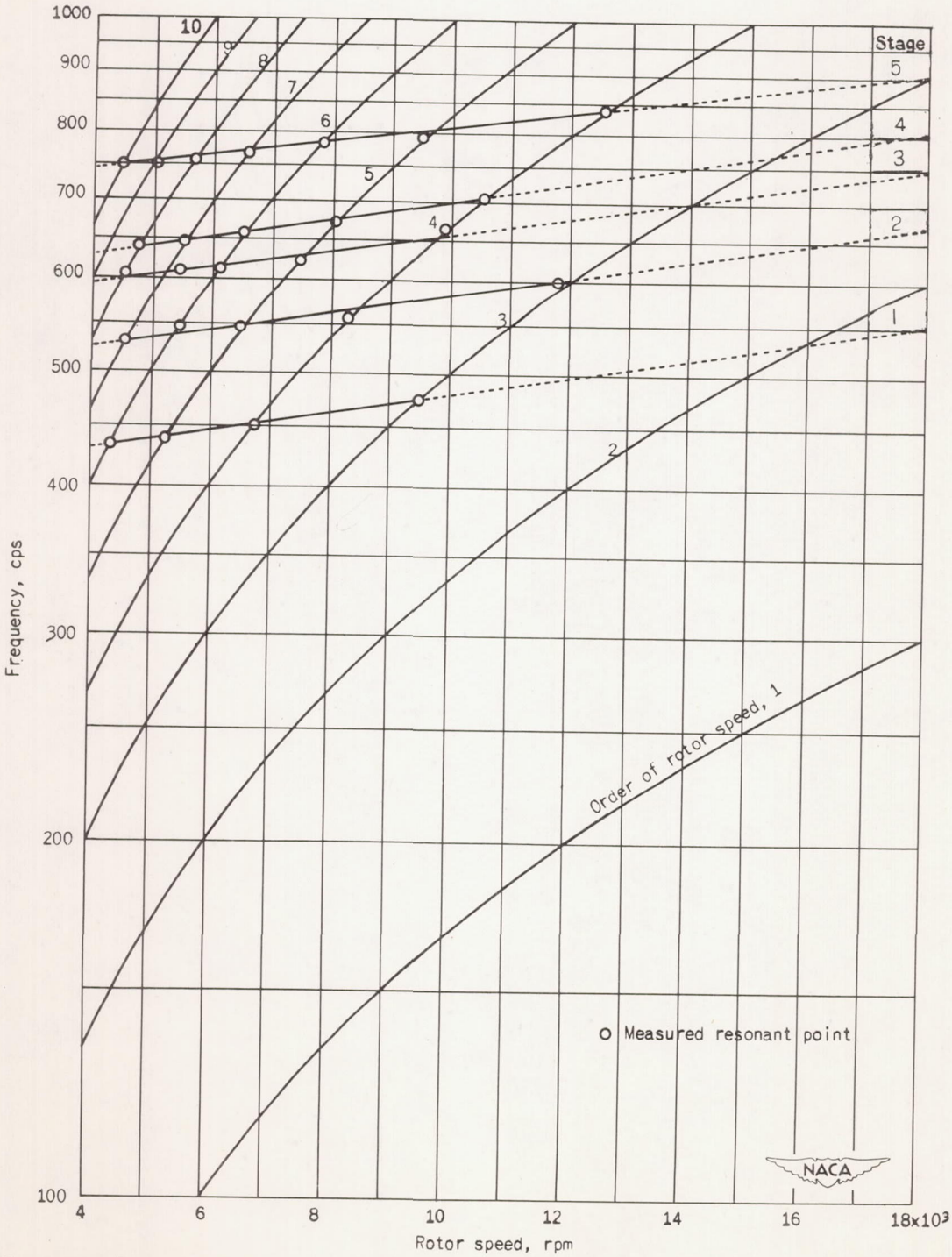

Figure 6. - Critical-speed diagram of 10-stage compressor showing only first bending-mode frequencies.

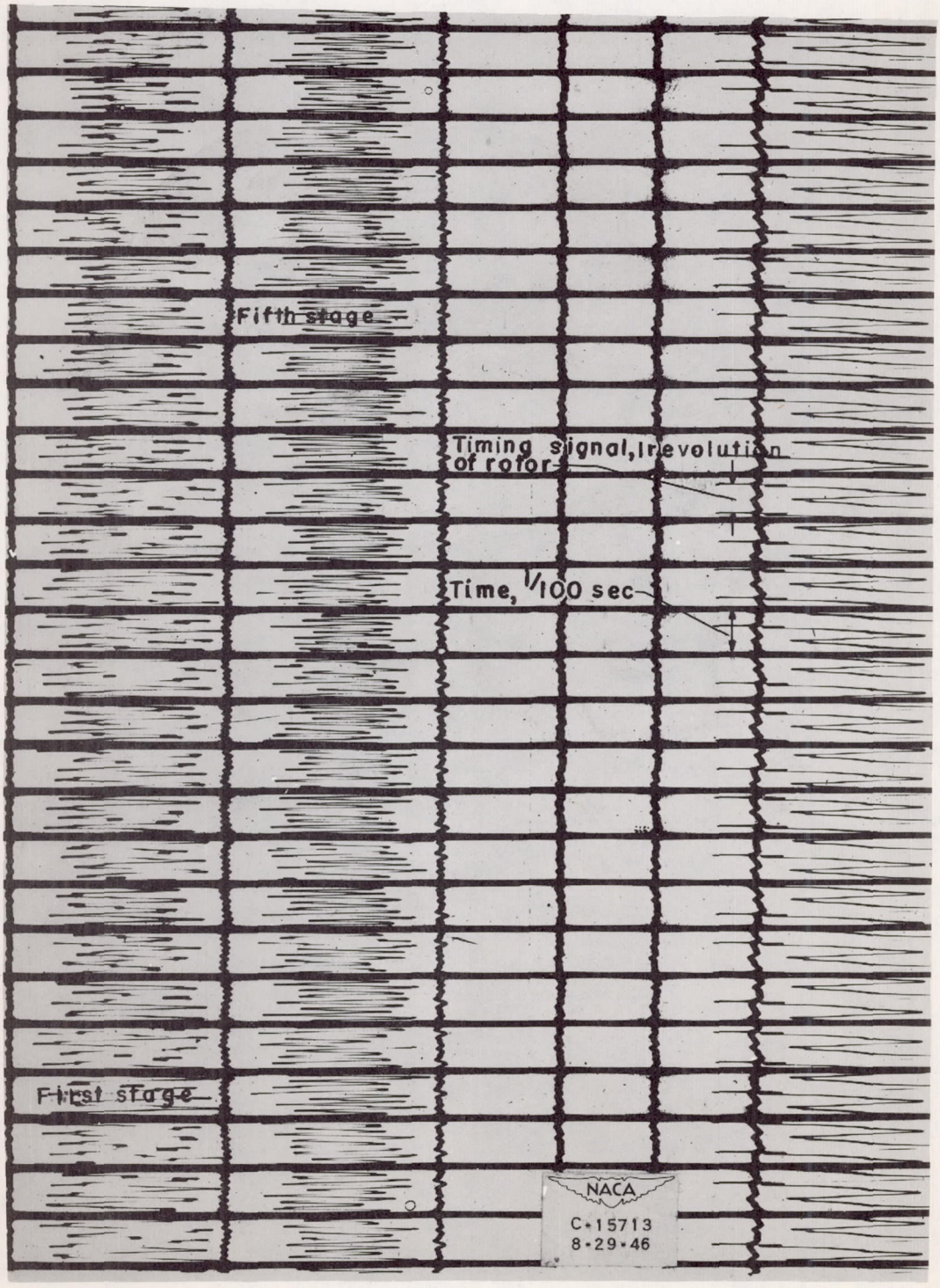

Figure 7. - Oscillograph record of representative strain-gage signals at rotor speed of 9485 rpm.

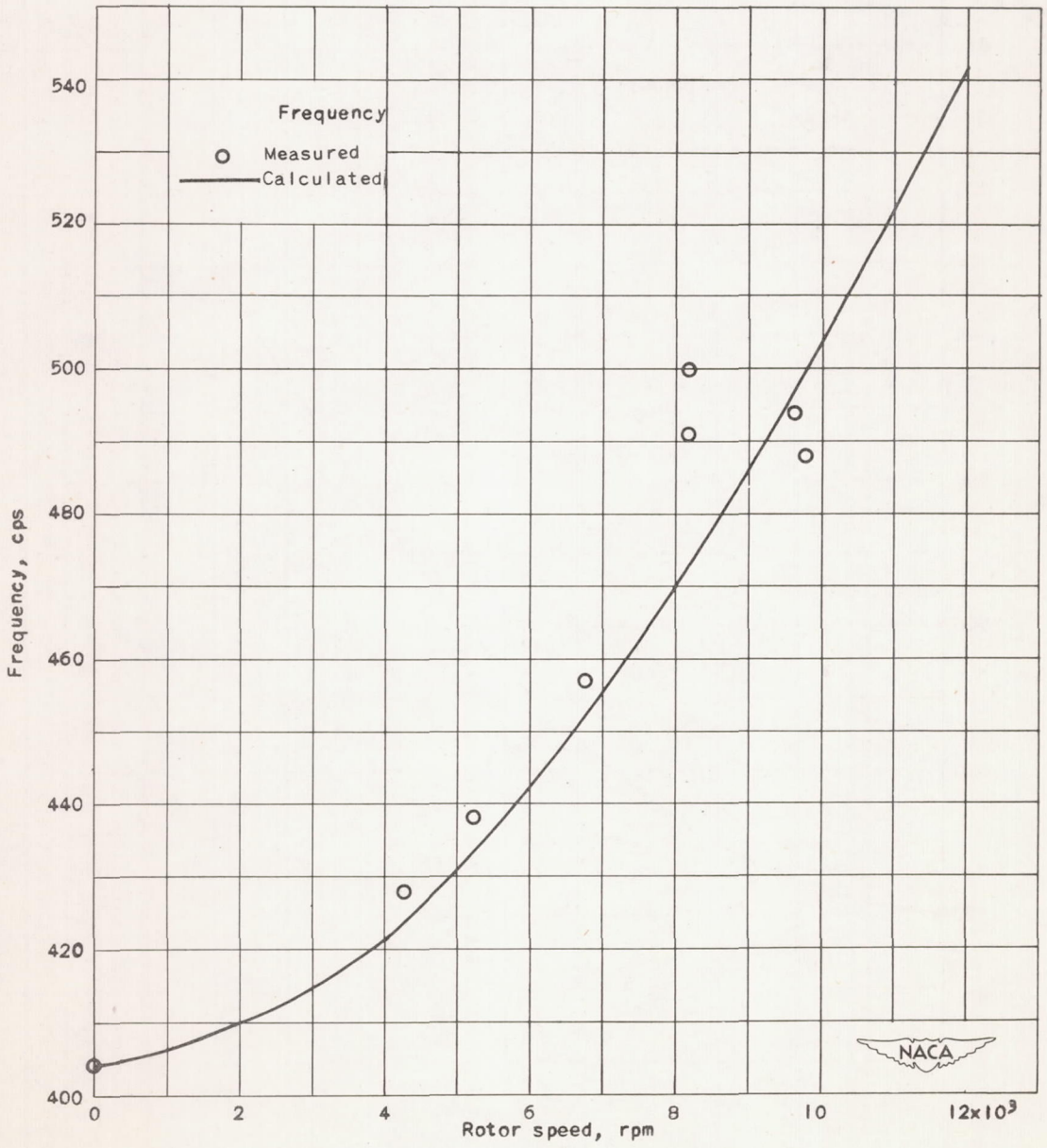

(a) First stage.

Figure 8. — Critical-speed diagram showing measured and calculated first bending-mode frequencies.

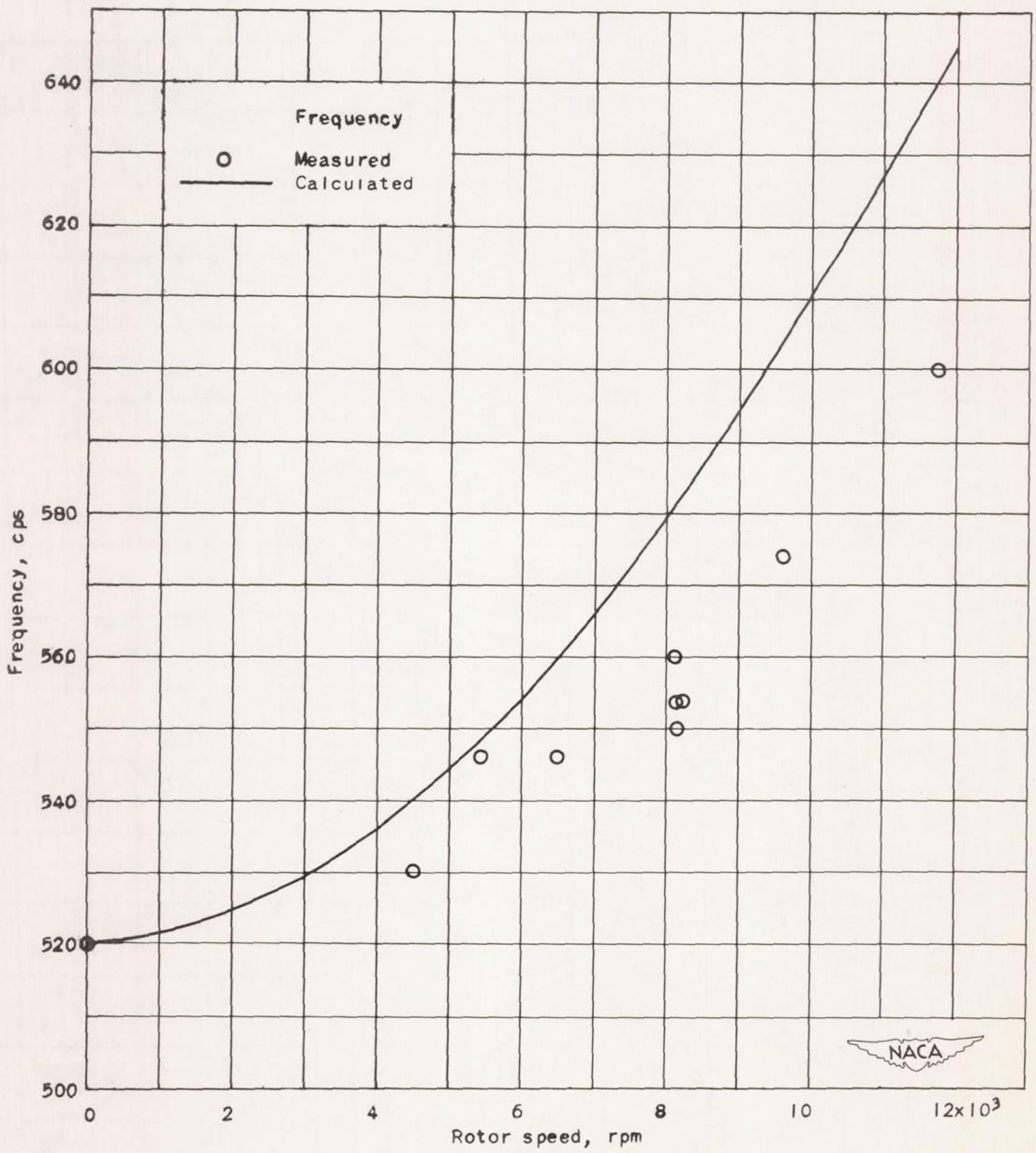

(b) Second stage.

Figure 8. – Continued. Critical-speed diagram showing measured and calculated first bending-mode frequencies.

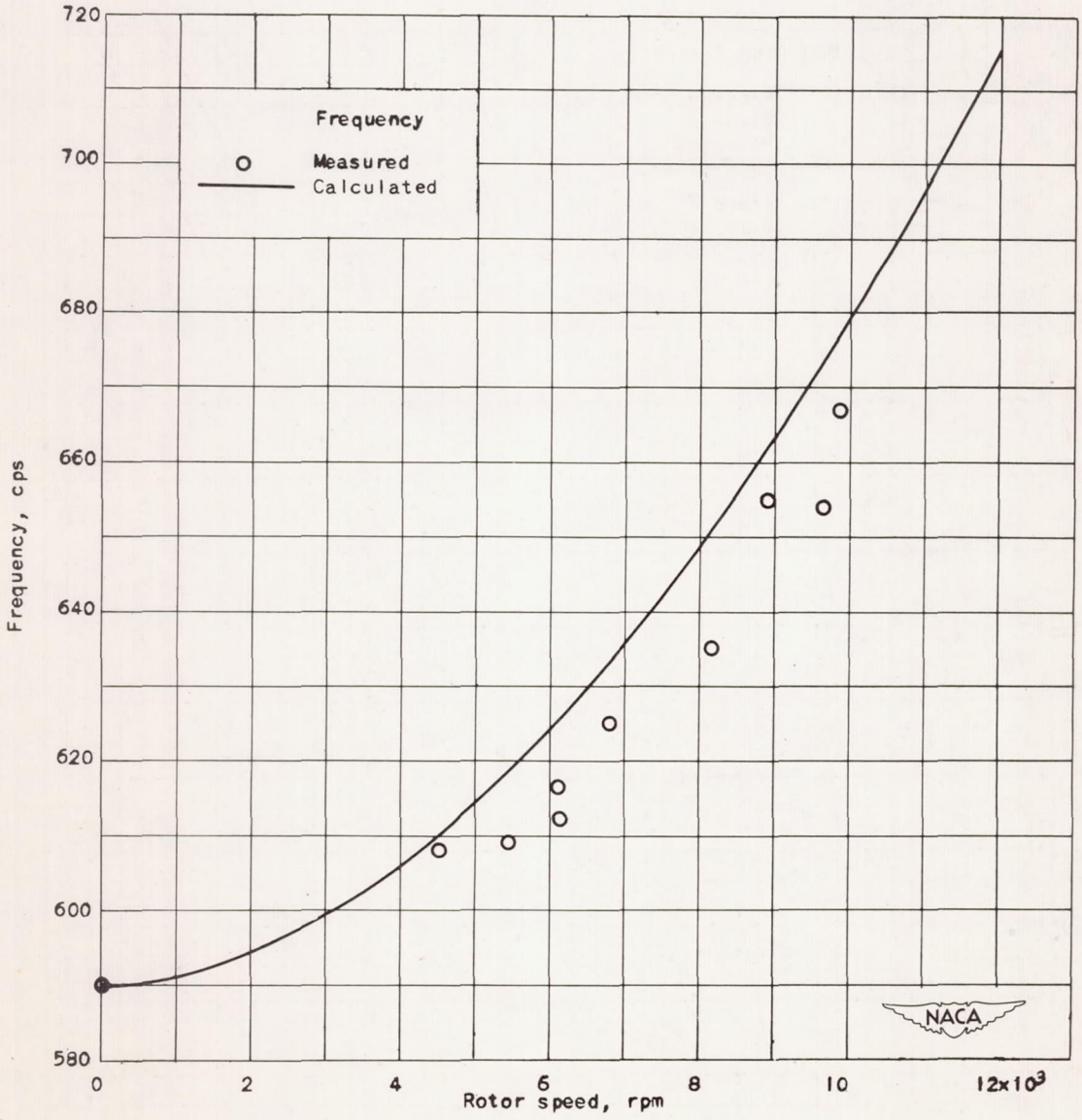

(c) Third stage.

Figure 8. - Continued. Critical-speed diagram showing measured and calculated first bending-mode frequencies.

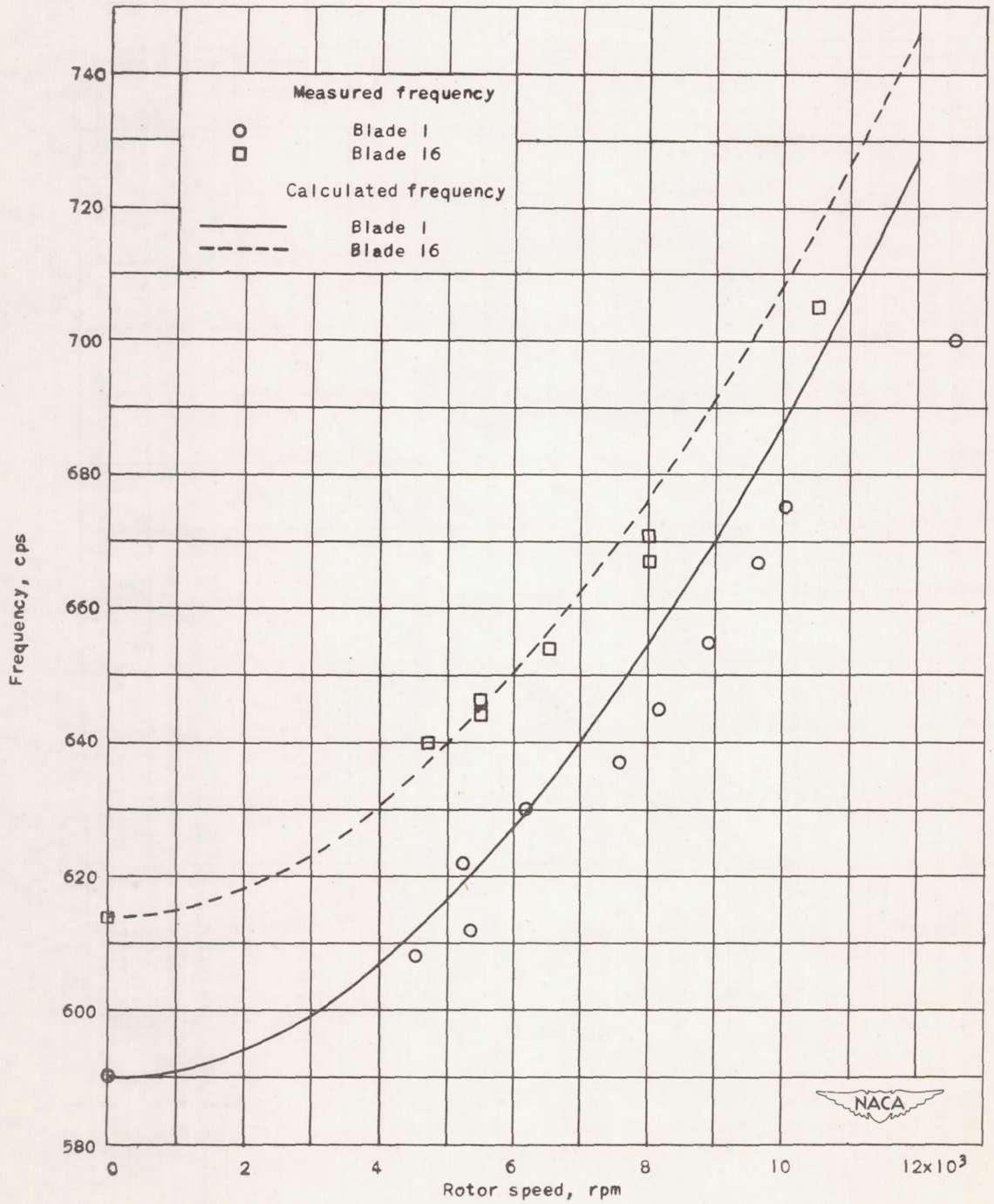

(d) Fourth stage.

Figure 8. - Continued. Critical-speed diagram showing measured and calculated first bending-mode frequencies.

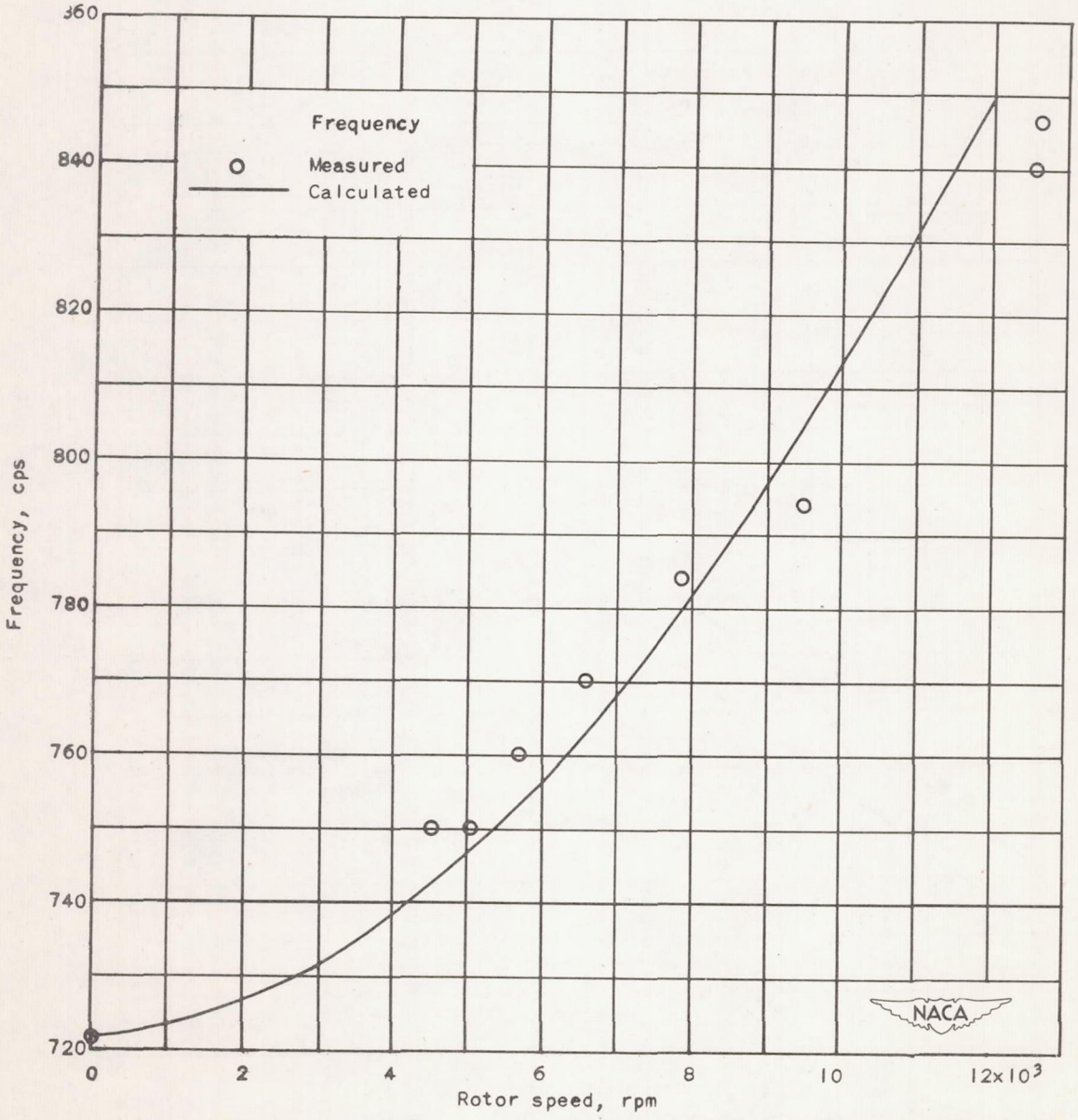

(e) Fifth stage.

Figure 8. – Concluded. Critical-speed diagram showing measured and calculated first bending-mode frequencies.

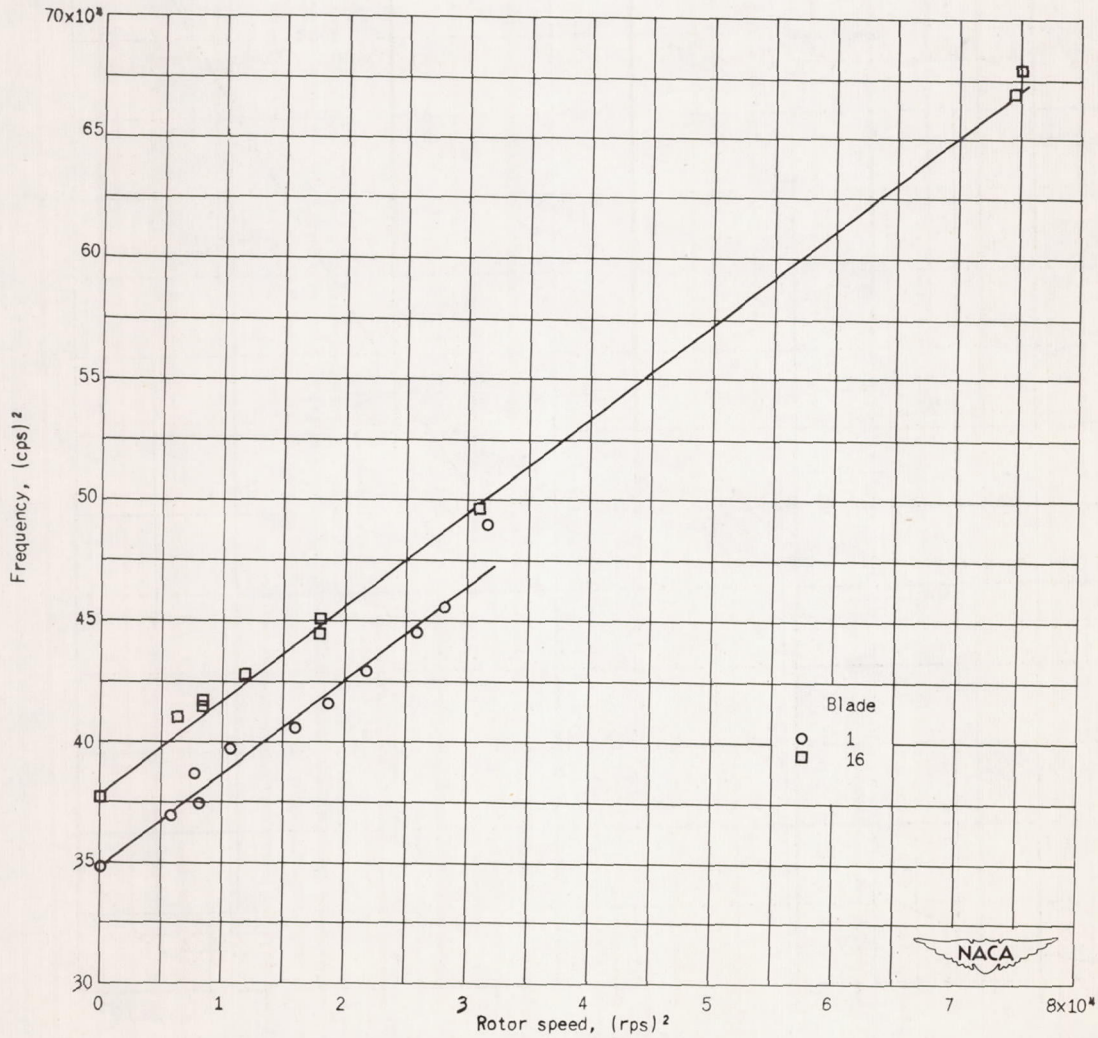

Figure 9. – Comparison of measured frequency with values calculated from static measurements. Fourth stage; first bending-mode frequencies.

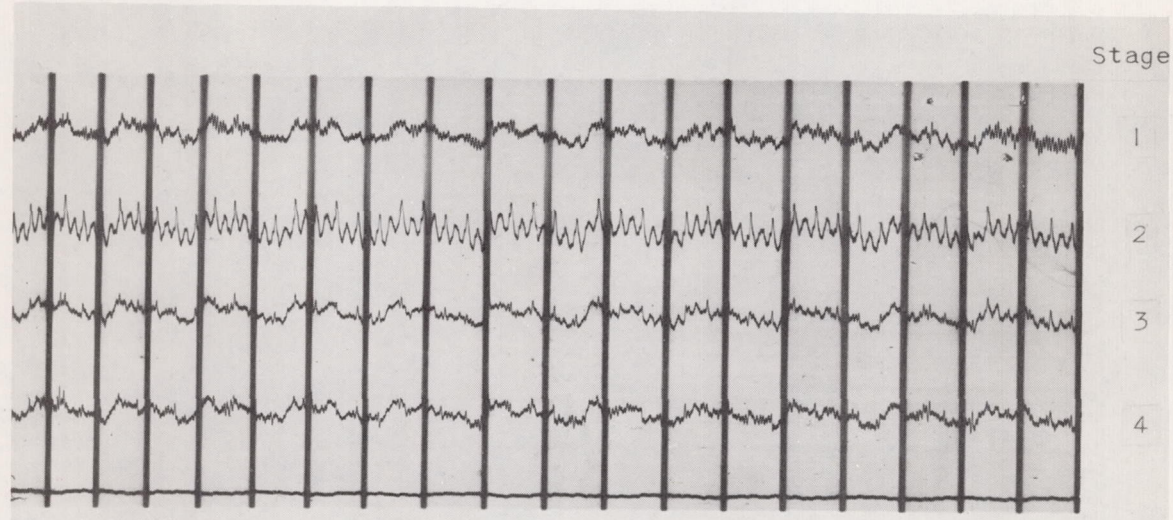

(a) Pressure ratio, 1.17.

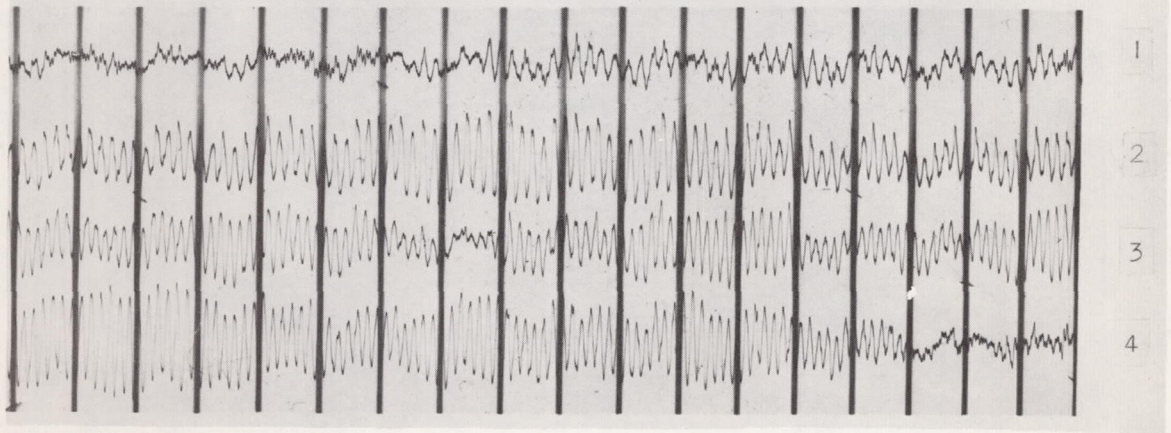

(b) Pressure ratio, 1.54.

NACA
C-18003
2-27-47

Figure 10. – Effect of varying pressure ratio at rotor speed of 8190 rpm.